CRACKING OF 304L STAINLESS STEEL OBSERVED WITHIN CANDU NUCLEAR POWER PLANTS UNDER CYCLIC MOIST ENVIRONMENTS

R. G. Allen, G. I. Ogundele, A. C. Lloyd, D. K. Jain, and A. K. Järvine
Kinectrics Inc., Ontario, Canada

Abstract

The stress corrosion cracking (SCC) of stainless steel Type 304L has been observed recently in a CANDU nuclear station. The cracking occurred on the inside surface of a piping structure and was transgranular in nature. It was mainly present in sections adjacent to welds, at pipe bends, and straight pipe sections. Such cracking mechanisms are governed by specific intrinsic parameters associated with stress, environment, and material factors. In this case, environmental factors are not typical for SCC, and, presumably, the operating stresses at the affected locations are low.

This paper discusses the results of the failure analysis conducted on affected component materials. The assessment of the observed mechanism includes the investigation of the affected piping (e.g., undamaged test welds, bends, and around the crack locations) using Orientation Imaging Microscopy to evaluate the relative degree of residual plastic strain present in the crack locations and in the general pipe microstructure. Advance surface analysis was used to examine metal surface oxides buried beneath deposits and at strained regions of the pipe in order to elucidate the chemical species likely involved in the cracking/degradation process.

1. Introduction

The CANDU (Canadian Deuterium Uranium) nuclear stations use natural uranium as fuel and deuterium oxide or "heavy water" as the moderator. The calandria vessel, two end shields, end shield supports, and the reactor shielding comprise the reactor assembly [1]. Within the low pressure low temperature moderator run the high pressure fuel channels. The moderator (heavy water) covers the reactor and above this a helium cover-gas system provides for normal pressure regulation within the calandria. The helium cover gas is recirculated for the removal of radiolytically produced deuterium and oxygen. Both the calandria and the cover gas relief ducts are manufactured from stainless steel type 304L (SS 304L). Shown in Figure 1 is a schematic diagram of the calandria shield tank assembly that illustrates the relationship of the calandria, shield tank, and cover gas relief ducts and piping to each other.

The normal operating temperature for the moderator cover gas (MCG) system is approximately 60ºC; the helium gas is saturated with D_2O vapour and contains less than 4% D_2 (which is the shut down limit) and 2% O_2 from radiolysis of D_2O. In units which can add oxygen a concentration of up to 3% is added so that deuterium reacts with the excess oxygen in the recombiners and is not allowed to build up. Typically the deuterium is <0.1% when

excess oxygen is added. The pressure of the helium cover gas inside the relief ducting is around 4 psig, which is quite low and internal pressure is not expected to impose stress on material during normal operating conditions.

2. Field observations

In January 2005, a significant increase in helium make-up supply flow rate was detected within the bulk helium supply system of a CANDU Nuclear Generating Station (NGS). A leak was suspected and traced to the MCG system in one of the units. Four months later, during a scheduled outage, personnel conducted a leak search on the system. Cracking was observed in the one-inch diameter (1″Ø) balance lines between two SS 304L 18-inch diameter (18″Ø) calandria relief ducts Y3 and Y4 in Figures 1 - 2.

In addition, the inside of one of the 18″Ø relief ducts was inspected and found to be discoloured and contained axial cracks as identified in the field using liquid penetrant inspection (LPI). The inspection revealed that the surfaces of the 18″Ø, schedule 40, 304L stainless steel duct were covered with brownish corrosion products with evidence of a condensation trail through the pipe and evidence of preferential weld corrosion (Figure 3). An array of axial cracks, oriented in the inside diameter of the 18″Ø relief duct directly below the attachment field weld between the shield tank and the outer diameter of the 18″Ø relief duct were visible. The appearance of the inside surface of the duct suggested that a contaminated and/or carbon steel grinding tool may have been used to grind the welds and other areas of the pipe surface during manufacture or installation. The use of carbon steel grinding tools can lead to a large quantity of Fe contamination in these areas, which is well known to cause significant corrosion of austenitic stainless steels.

The observed cracking necessitated a more comprehensive examination of the samples and initiated the investigation into the cause of the failure. It is well recognized SCC is influenced by a number of interrelated variables with the principal factors being the combination of a susceptible material subjected to a local tensile stress and exposed to a specific corrosive environment. These aspects were examined in the ensuing examination of the sections that were available for analysis.

This paper presents preliminary information on a work-in-progress on the assessment of the degradation observed. These include metallographic examination, evaluation of residual stresses in samples removed from the field, and surface analysis of field samples.

3. Laboratory Metallographic Examination

The cracked 2″ x 1″ reducer and a section of the 1″Ø pipe were removed for examination; extensive circumferential through-wall cracks were observed on the 1″Ø pipe (Figure 4) and the cracking in the 1″Ø pipe was through-wall where the pipe was welded to the reducer. The major crack was located on the 1″Ø pipe just downstream of the weld to the reducer. The pipe was cut open axially to reveal the ID surface where the corrosion indications extended well beyond the weld into the bend and straight sections of the pipe. Brownish-coloured corrosion deposits

appeared throughout the ID surface of the pipe, which corresponded to dark brown cracks and small localized spots along the sectioned crack. In the 1″Ø pipe, the cracking concentrated in the bends, suggesting that residual stresses from bending contributed to the SCC. As evident in the cross-section (Figure 4), the cracking initiated from the inside surface of the pipe and propagated (with some branching) in a transgranular manner, leading to through-wall failure of the pipe and the resulting increase in the helium consumption observed in the station.

Since it was impractical to remove the section of the 18″Ø duct containing the cracks, an extensive metallurgical examination (similar to those conducted on the 1″Ø pipe) could not be performed. Field UT examination suggested that the depth of the crack in the duct was 20 % through-wall. Field liquid penetrant inspection (LPI) revealed the presence of axial cracks on the inside surface of the 18″Ø pipe. Information regarding the material and nature of the cracking observed in the 18″Ø pipe was obtained from replicas of the axial cracks, analysis of the corrosion deposits, hardness measurements, and microsampling. A section of the replica image is shown in Figure 5. The data from replication indicated that the cracking observed in the 18″Ø pipe had propagated in a transgranular manner, similar to the cracks on the 1″Ø pipe. The nature of the cracking suggests that these cracks likely initiated and propagated by the same mechanism as that for the 1″Ø pipe. Multiple, axially oriented cracks were evident in the areas sampled. Some of these cracks are stepwise in nature, while some had coalesced to form longer cracks.

The chemical composition of the 1″Ø pipe as well as hardness measurements from the 1″Ø pipe and 18″Ø duct (Table 1) was collected. The composition results confirmed the material is in conformity with required material specifications for austenitic stainless steel type 304L (85-88 HRB). The hardness of the MCG material in the cracked regions of the 1″Ø pipe (97 HRB) is higher than that measured for the ‘bulk’ pipe material at locations away from any cracks or welds (83-88 HRB). The slightly higher hardness is an indication of the presence of residual strain in the material at the location sampled. This suggests that if post welding stress relief of the 1″Ø pipe was carried out, it was not adequate to remove the residual stresses, ultimately rendering the material to be susceptible to cracking at the affected areas of the pipe.

4. Residual Strain Distribution Using Orientation Imaging Microscopy

Orientation imaging microscopy (OIM) was used to characterize the residual plastic strain distribution present within cracked areas and around the cracked weld between the 1″ x 2″ reducer to 1″Ø pipe. An area where severe ID-initiated cracking was found (Figure 6a,b) was sectioned axially, clearly displaying the multiple cracks. A significantly high level of residual strain was observed in the crack tip area, indicating that the crack could continue propagating. Elevated residual strain was also observed along the inside surface of the crack (Figure 6c) indicating that the crack had propagated through a highly strained area so that the internal stress was released. This can be compared to a sample of un-cracked material, in which the residual plastic strain of the material is uniformly distributed and is at low levels (Figure 6d). These results correlate with the elevated hardness measurements obtained, as discussed above.

5. Assessment of Environmental Influences using Surface Analysis

A significant factor in the initiation and propagation of stress corrosion cracking in 304L stainless steel is the environmental chemistry. To ascertain the operating chemistry conditions, analysis of the deposits and oxides on the surface in affected regions of the material was conducted using Secondary Ion Mass Spectroscopy (SIMS) depth profiling. This allows information on the variation of composition with depth below the initial surface of the oxide layer to be obtained, revealing the depth distribution of impurities present with a detection limit in the ppb to ppm levels.

The composition of the oxide deposit on the 18″Ø duct was assessed by taking micro samples approximately 0.008″ thick from the inside pipe surface in both unaffected (e.g., grey-coloured surface) and affected (e.g., rust-coloured surface) regions of the pipe. Typical examples of the scrape samples are provided in Figure 7. The smooth, shiny backside surface indicates that the scrape samples were deep enough to penetrate through to the bulk pipe material.

In the SIMS depth profiles obtained for the 18″Ø duct for Cl (Figure 8) the rust coloured areas show the most intense Cl profiles and therefore contain the highest concentration of Cl compared to both the grey-coloured areas and the backside of the scrapes (e.g., base metal). The Cl detected on the backside of the scrape samples was likely introduced during sampling and handling. Chloride is found in higher concentrations and extends deeper into the oxide near the regions that exhibited discolouration or were there is evidence of corrosion product accumulation on the surface. This suggests that Cl is concentrated in localized regions on the 18″Ø pipe. The depth profiles in rust coloured regions display a smooth decrease with time (e.g., oxide depth) in the Cl profiles through the sample approaching the oxide/metal interface. This suggests that Cl in the affected areas was incorporated into the indigenous oxide and thus had built up since the plant went into operation.

6. Discussion

The cracking observed in the 1″Ø and 18″Ø pipes has been shown to have occurred in a transgranular manner in the presence of brown-coloured corrosion deposits and in the presence of chlorides. Additionally, the cracking appears to have occurred in regions of high residual strain, with likely crack growth evidenced by the high level of residual strain observed in the crack tip area. In both pipes, there were contributions from the piping material, the environmental chemistry, and fabrication stresses. The piping material in the affected CANDU unit had been in service for 18 years before the failure was discovered.

As in every degradation mechanism observed in a component, it is difficult to implicate a single factor as being the main cause without considering the synergistic effect of other likely contributors. In this particular investigation, the role of the environmental chemistry is considered to be significant. Given the unusual circumstance that the degradation occurred, some possible scenarios were considered below. These are chloride activity, discolouration, effect of oxygen, and residual stresses.

Chloride activity: In the system under consideration, the humidity was very high and the amount of was chloride (presumably) low. Most practical cases of SCC occur on hot surfaces where the local relative humidity (RH) value is relatively low so that highly soluble salts can form highly concentrated solutions. However, if the chlorides are present within a tight creviced area, then relatively dilute chloride solutions can initiate SCC. Low levels of chlorides initiating cracking can be rationalized using the approach of Sato and Tsujikawa [1, 3] who showed that a rust layer can act as a crevice by creating an anion-selective membrane. The creation of such a membrane creates a region of stable localized pitting and is especially effective at very low chloride concentrations [4]. Stress corrosion cracking is known to initiate from sites where stable, localized corrosion is occurring and a crevice or tenacious deposit needs only a dilute solution of chloride.

In the MCG gas system, the relative humidity was high in the outlet relief ducts, such that only dilute chloride solutions could have existed on the surface. Thus, high concentrations of Cl were likely the result of the formation of an adherent deposit. The results of the current examination suggest that, in some cases, the cracks initiated at pit sites or in the vicinity of corrosion deposits, which may have acted as a stable trap for chlorides. The presence of only a thin film of electrolyte, which allows for easy access of oxygen to the metal surface, thereby creating more oxidizing (aggressive) conditions is one way that this stabilization can occur. Additionally, contamination of the austenitic stainless steel surface with iron oxides, which act as anion-selective membranes that can promote stable pitting, is another corrosion-accelerating factor, and has likely occured for the MCG system under investigation.

Discolouration of the surface: The corrosion resistance of stainless steel is imparted by the formation of a protective oxide film on the surface. This film is principally Cr_2O_3 and is generally a shiny grey colour. The inspections of the relief duct show that over largely all the duct surface, the pipe surface had lost this lustery appearance and revealed affected areas that had rust deposits and localized corrosion. The visual appearance of the inside surface suggests that a contaminated and/or carbon steel grinding tool was used to grind the welds and other areas of the pipe surface during manufacture or installation. The use of carbon steel grinding tools can lead to a large quantity of Fe contamination in these areas, which is well known to cause significant corrosion of austenitic stainless steels. This is a well-known form of corrosion initiation for SS, which occurs when carbon steel grinding tools or brushes are used on a SS surface. Additionally, when iron contamination is present (either from an external component or grinding of the surface with carbon steels) localized spots with rust deposits can be initiation sites for pitting. These rough areas could conceivably trap chlorides, contributing further to the pitting. In the Unit in question both chloride and the appearance of ground, rough surfaces was observed.

Effect of oxygen: The presence of small amounts of oxygen in the MCG environment (introduced during outages, etc.) may exacerbate the problem. A thin layer of moisture (condensate) readily allows oxygen to diffuse to the metal surface. The results of surface analysis suggest that Cl and O are concentrated in those areas that show cracking or significant corrosion products (discolouration of the surface). Oxygen can induce stress corrosion cracking in Cl-containing media because pitting occurs when it is present. Another contributing factor is a shift of the corrosion potential in the presence of oxygen, to values that are noble to the critical potential for stress corrosion cracking. For this situation, stress corrosion cracking can occur

regardless of whether corrosion pits develop [5]. This was the likely scenario in areas where cracking was observed without pitting.

Residual stresses: Manufacturing stresses are possible contributors to the initiation and propagation of transgranular SCC. At welds, the driving force would be related to the residual stresses from the field weld process and any pre-existing fabrication-induced stresses from manufacturing. The relative residual strain levels within grains present in the microstructure of the 1″Ø pipe in the vicinity of a crack were assessed and revealed that the strain level along the cracks is slightly higher than that in the vicinity of the crack. This suggests that the preferential cracking at the bend occurred due to higher localized residual stress from bending. The cracking that occurred on the 18″Ø relief duct was in the vicinity of the circumferential weld to the shield tank collar, although there were also associated grinding marks in the weld area. It is also expected that the SCC in this region of the 18″Ø duct is due to installation-related stresses, although this could not be confirmed in the current investigation.

7. Conclusions

The degradation of SS 304L components in the CANDU MCG piping can be attributed to SCC. From the preliminary assessment, it was shown that the failure of the stainless steel type 304L 1″Ø pipe and axial cracking of the 18″Ø relief duct piping was due to Cl induced transgranular stress corrosion cracking. The sequestering of chlorides in localized areas of the piping led to cracking where residual stress existed and staining and pitting in those regions where it did not.

The localized accumulation of chlorides is hypothesized to be due to the synergistic effects of iron oxide contamination (possibly by the use of a carbon steel grinding tool during installation) and the moist environment of the moderator cover gas system. Efforts to understand the SCC susceptibility of austenitic 304L stainless steel in pertinent environments and to identify the main contributing factors in the cracking are ongoing.

8. References

1 “Assessment and management of ageing of major nuclear power plant components important to safety: CANDU reactor assemblies”, IAEA-TECDOC-1197 (February 2001).
2 N. Sato, "Some concepts of corrosion fundamentals”, Corrosion Science, Volume 27, No. 5, pp. 421 - 433 (1987).
3 S. Tsujikawa, “Initiation of Cl SCC cracks from crevices rather than from pits” Chemistry and Electrochemistry of Corrosion and Stress Corrosion Cracking, pp. 339 - 349 (2001).
4 M. Suleiman, I. Ragualt, and R. Newman, “The pitting of stainless steels under a rust membrane at very low potentials”, Corrosion Science, Volume 36, pp 479 - 486 (1994).
5 P. A. Andresen and D. J. Duquette, “The Effects of Dissolved Oxygen, Chloride Ion and Applied Potential on the SCC Behavior of Type 304 Stainless Steel in 290°C Water”, NACE, Volume 36, No. 8, pp. 409 - 415 (1980).
6 Provided by AECL-Sheridan Park, as drawn by Aldo Aceto, Simulation Technologist.

Acknowledgements

The authors would like to acknowledge the involvement of Bruce Power Station personnel; specifically: Jim Beaton and Bikash Chatterjee.

Table 1: Hardness of the material within the MCG system

Sample	Hardness (HV)	Hardness (HRB)
1″Ø pipe away from the weld	144 – 165	77 – 84
1″Ø pipe near the weld, not near crack	164 – 183	83 – 88
1″Ø pipe crack tip	175 – 230	97
18″Ø duct in cracked region	171 – 189	85 – 90
ASME Specification for 304L SS	176	88 (max)
Mill Certificate	165	85

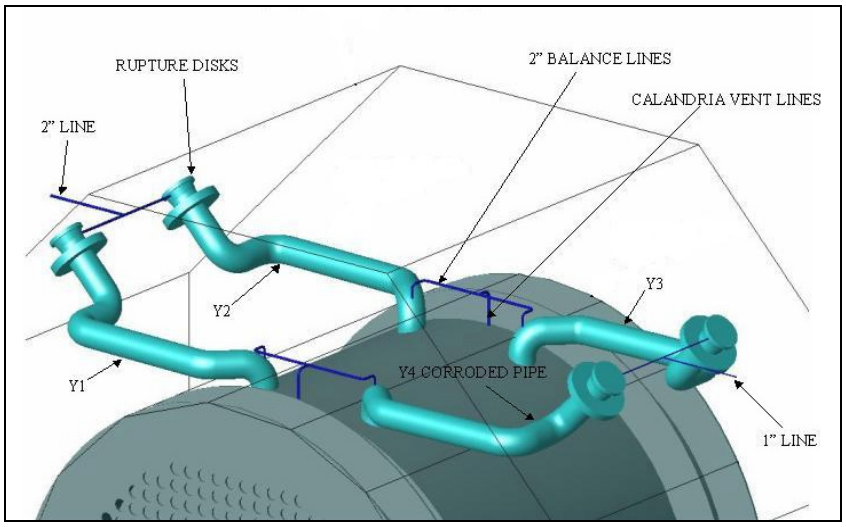

Figure 1: Schematic diagram of the calandria shield tank assembly, illustrating the relationship of the calandria, shield tank, and cover gas relief ducts and piping to each other [6].

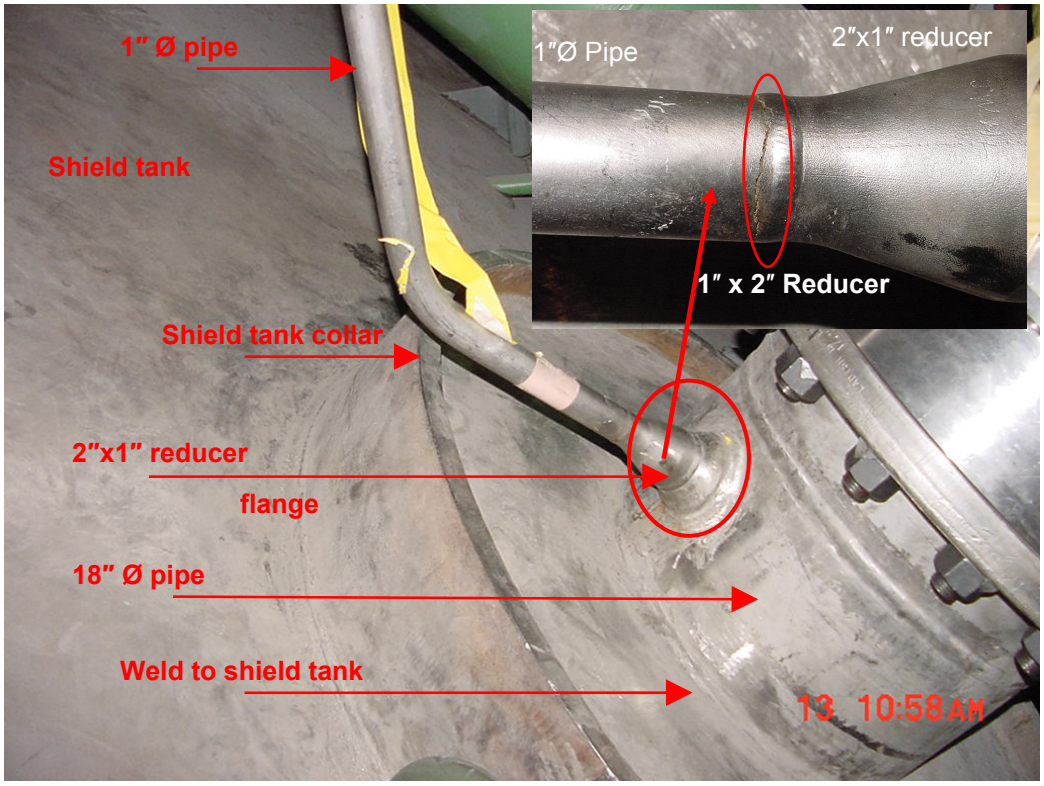

Figure 2: Photograph of the 1″Ø pipe and 18″ relief duct.

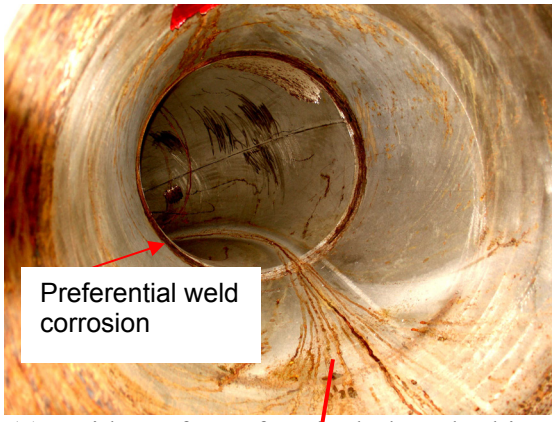

(a) Inside surface of 18-inch duct, looking down the duct

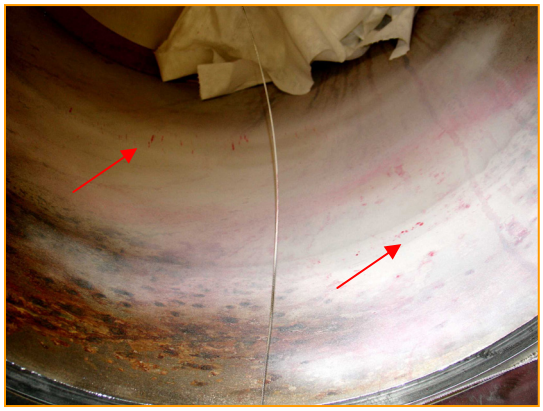

(b) Liquid penetrant inspection (LPI) found axial crack-like indications

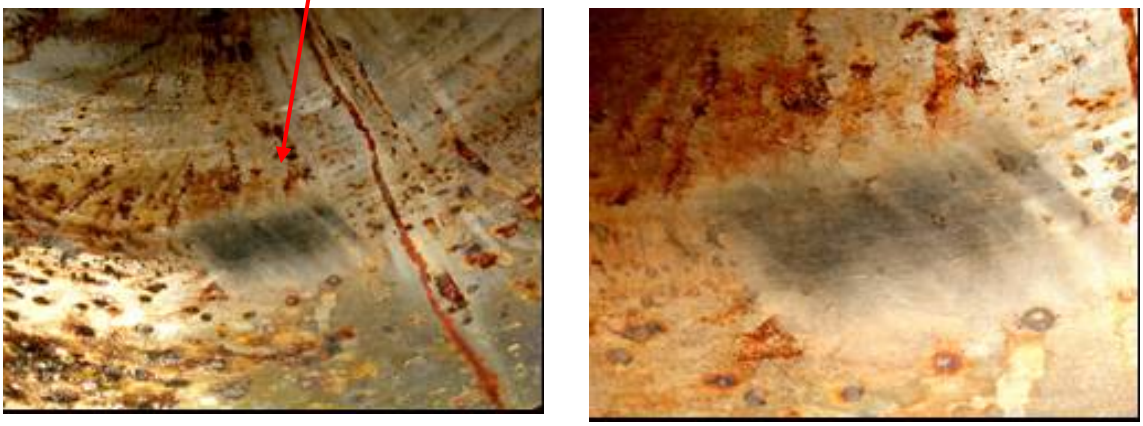

(c) Area scraped for deposit examination

Figure 3: Photographs illustrating the typical corrosion pattern on the inside surface of the 18″Ø relief duct piping below the flange in the affected unit.

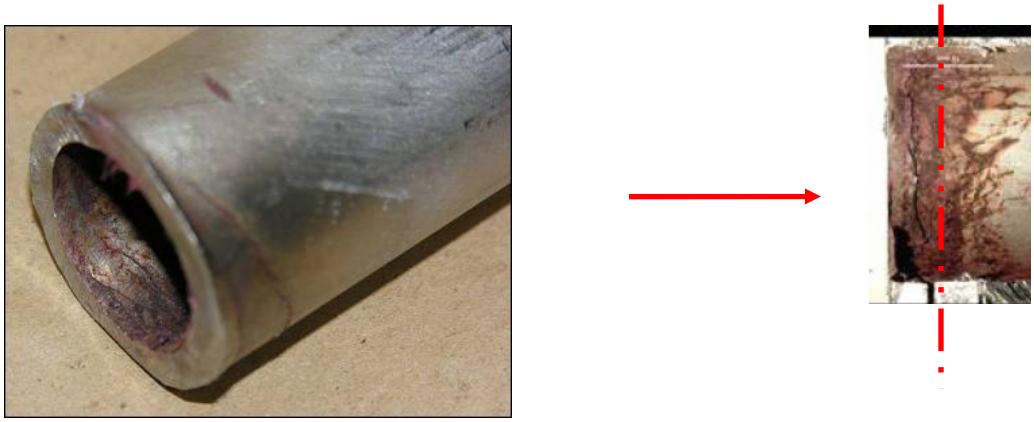

(a) 1″ Ø pipe showing the cracking (b) Cut for mount, polishing direction shown

OD

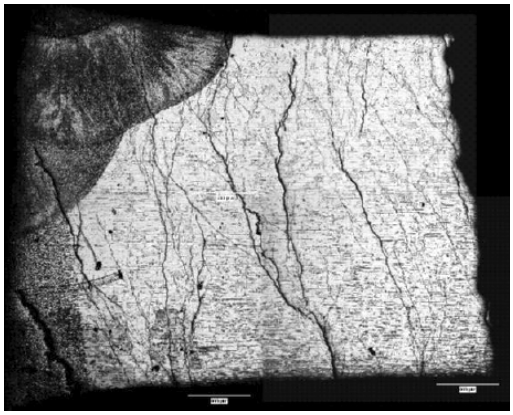

ID

(c) Mounted and etched cross section

Figure 4: Cracking observed in the 1″ Ø pipe (through the cracked region of the 1″Ø pipe just downstream of the weld to the 2″X1″ reducer). The cracking appears transgranular and ID-initiated.

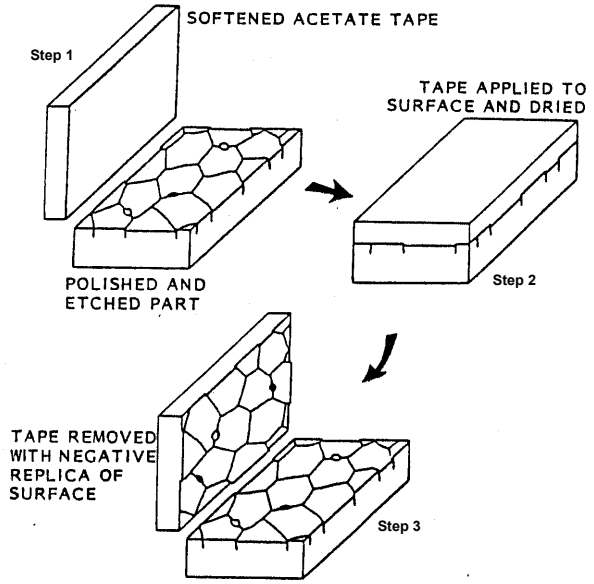

(a) Schematic diagram of the replication process

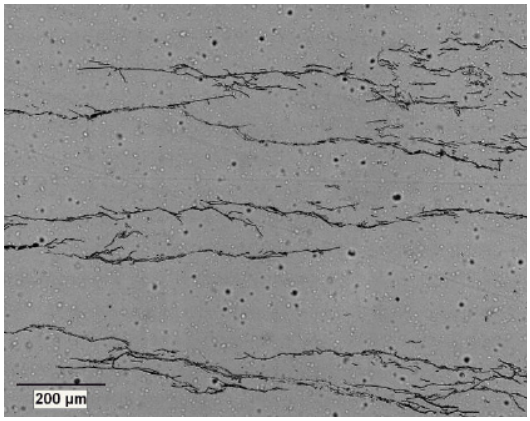

(b) Part of the axial crack

Figure 5: Replica images of the axial cracks on the inside surface of the 18″ Ø relief duct piping; these images were taken on the ID of the 18" duct directly below attachment weld to shield tank wall on the OD of the duct (as shown in Figure 1).

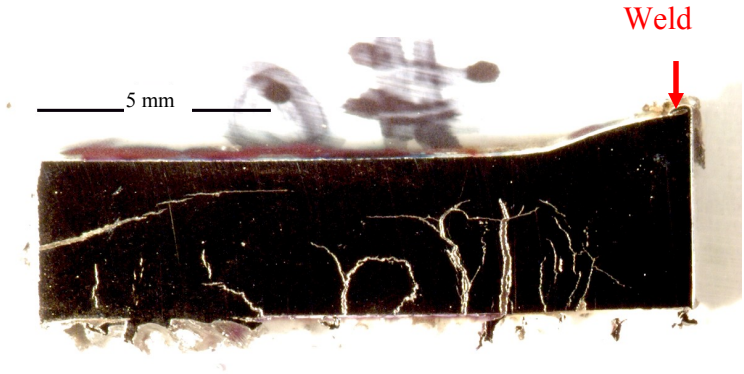

ID surface side

a) Optical image of the sectioned crack

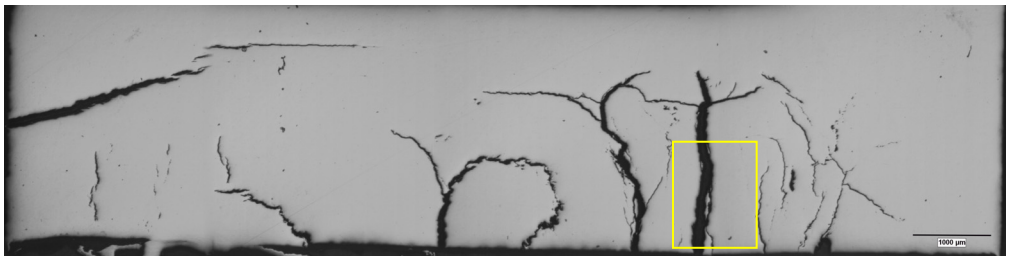

ID surface side

b) Metallographic sample of the sectioned crack

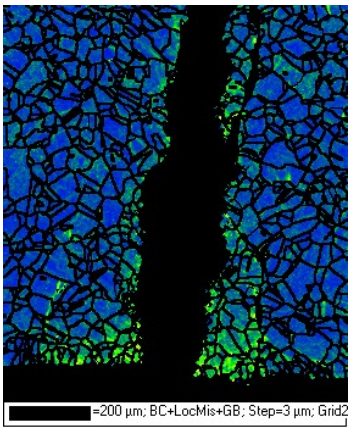

c) Strain map of location indicated in (b)

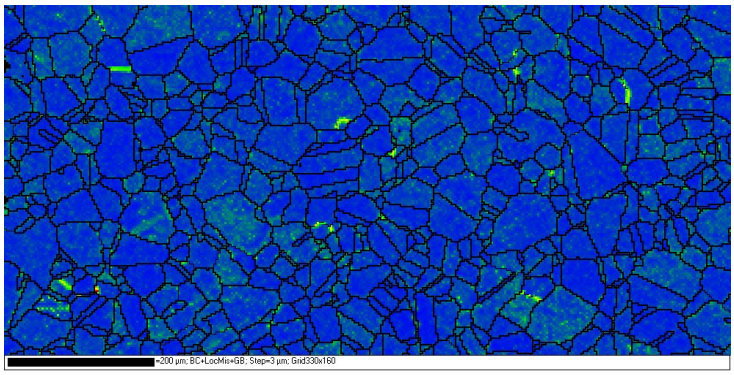

d) Strain map of un-cracked location

Figure 6: Strain map of a random selected area on an axially sectioned and polished sample of the 1″Ø moderator cover gas pipe.

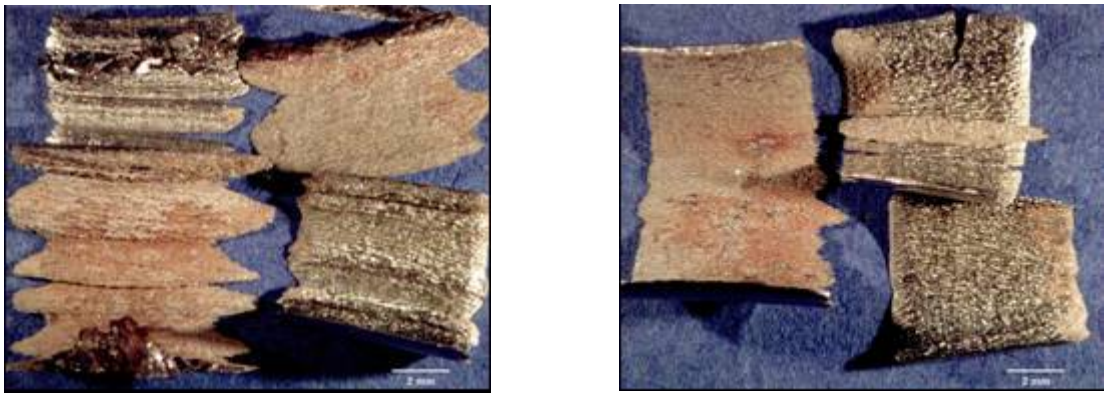

(a) affected (rust-coloured) and unaffected (grey-coloured) scrape samples

(b) backside of a scrape sample

Figure 7: Micro-sampling (scrape) samples from the 18″Ø duct.

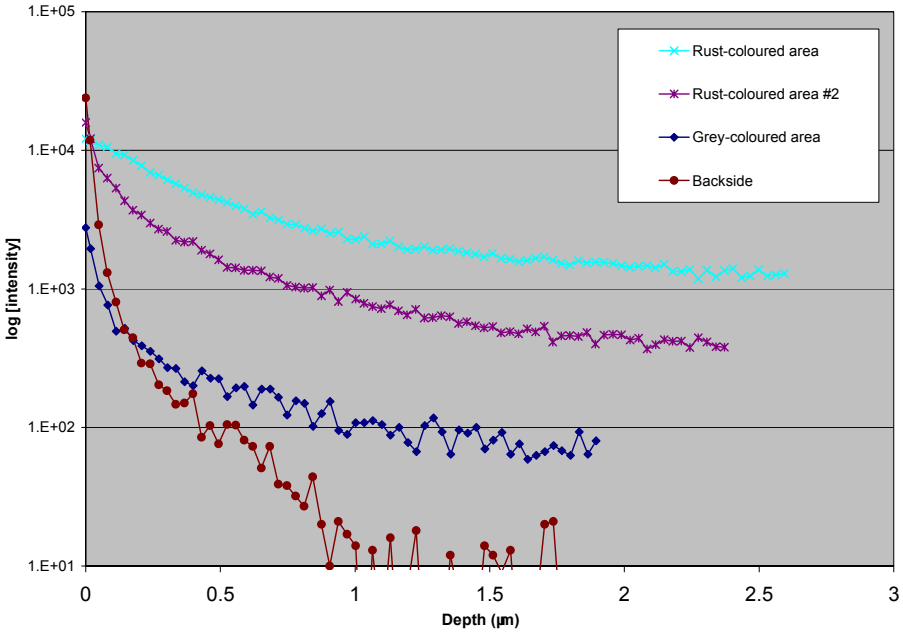

Figure 8: Chlorine SIMS depth profiles for scrape samples from the 18″Ø duct.